JOURNAL OF GEOPHYSICAL RESEARCH, VOL. 113, A10214, doi:10.1029/2008JA013284, 2008

Anomalous geomagnetic storm of 21–22 January 2005: A storm main phase during northward IMFs

A. M. Du,[1] B. T. Tsurutani,[2] and W. Sun[3]

Received 8 April 2008; revised 10 June 2008; accepted 28 July 2008; published 28 October 2008.

[1] The major (minimum Dst = −105 nT) magnetic storm which occurred on 21–22 January 2005 is highly anomalous because the storm main phase (identified by the SYM-H indices) developed during northward interplanetary magnetic fields (IMFs). We believe this to be the first event of its type to be reported in the literature. Interplanetary ACE and Cluster C1 data are used for solar wind diagnostics, and LANL 90 and 97, GOES 10 and 12 and GEOTAIL data are used for magnetospheric diagnostics. An unusually strong (magnetosonic Mach number equal to 5.4) shock detected at ∼1647 UT, 21 January 2005 by ACE causes a SI+ (of 57 nT) at ∼1712 UT at Earth. Southward magnetic fields in the sheath following the shock caused a decrease of SYM-H with a peak value ∼−41 nT. A dynamic pressure jump across a double discontinuity in the solar wind at 1823 UT observed by ACE induced a second SI+ (of 25 nT) at 1847 UT at Earth. Southward magnetic fields following this event led to a second SYM-H decrease with peak intensity −2 nT. However, when the storm main phase developed starting at 1946 UT, the IMF Bz turned northward. The IMF was northward from the portion of the main phase from ∼1946 UT to 0124 UT (almost 6 h). By comparing solar wind energy input (represented by integrated interplanetary *Ey*) with accumulated energy in the ring current (represented by integrated SYM-H), we arrive at a possible explanation that there is first energy storage in the magnetotail and then a delayed energy injection (after storage in the magnetotail) into the magnetosphere. Other interpretations/mechanisms are possible.

Citation: Du, A. M., B. T. Tsurutani, and W. Sun (2008), Anomalous geomagnetic storm of 21–22 January 2005: A storm main phase during northward IMFs, *J. Geophys. Res.*, *113*, A10214, doi:10.1029/2008JA013284.

1. Introduction

[2] The characteristic signature of a geomagnetic storm is a depression in *H* component of the Earth's near-equatorial magnetic field lasting from ∼1 to up to ten hours [*Kamide et al.*, 1998]. This depression is primarily caused by the westward (diamagnetic) ring current encircling the Earth [*Feldstein et al.*, 2005]. The Dst or SYM-H indices, as a measurement of the ring current [*Gonzalez et al.*, 1994], are well-correlated with the solar wind-magnetosphere coupling functions such as epsilon [*Akasofu*, 1981a, 1981b], and the solar wind dawn-dusk electric field [*Burton et al.*, 1975; *Gonzalez and Tsurutani*, 1987; *Gonzalez et al.*, 1989, 2007]. A main phase of the storm typically follows the intense long-duration southward IMF field with a delay of ∼1 h [*Tsurutani et al.*, 1988; *Kamide et al.*, 1998; *Gonzalez et al.*, 1994].

[3] Interplanetary coronal mass ejections (ICMEs) [e.g., *Tsurutani et al.*, 2004], corotating interaction regions (CIRs) [*Smith and Wolfe*, 1976] and Alfvenic IMF fluctuations are the main sources leading to the development of the magnetic storms [*Kamide et al.*, 1998]. Owing to the strong empirical relation between southward magnetic fields and magnetic storms it is assumed that magnetic field merging [*Dungey*, 1961] is the principal mechanism for energy transfer between the solar wind and the magnetosphere [*Gonzalez et al.*, 1994, 2007; *Echer et al.*, 2008a, 2008b].

[4] Besides magnetic reconnection, "viscous interaction" [*Axford and Hines*, 1961] has been suggested to explain solar wind energy transfer. One specific mechanism of viscous interaction is cross-field plasma diffusion from the magnetosheath to the magnetopause boundary layers by resonant wave-particle interactions [*Tsurutani and Thorne*, 1982]. Another is the Kelvin-Helmholz instability [e.g., *Lamb*, 1945]. However, *Echer et al.* [2008b] note that none of these caused magnetic storms of intensity Dst < −100 nT during solar cycle 23.

[5] It has been shown that during intense northward interplanetary fields, the solar wind coupling efficiency is typically two orders of magnitude below that during magnetic reconnection intervals such as those causing intense substorms and storms [*Tsurutani and Gonzalez*, 1995]. The August 1972 interplanetary event had the highest solar wind

[1]Institute of Geology and Geophysics, Chinese Academy of Sciences, Beijing, China.
[2]Jet Propulsion Laboratory, California Institute of Technology, Pasadena, California, USA.
[3]Geophysical Institute, University of Alaska Fairbanks, Fairbanks, Alaska, USA.

0148-0227/08/2008JA013284$09.00

speed (Vsw > 1500 km.s) ever detected at 1 AU and was characterized by an intense northward magnetic cloud embedded within a complex field and plasma structure [*Tsurutani et al.*, 1992]. *Tsurutani et al.* [1992] interpreted this event which had 3 southward magnetic field intervals and the northward MC as causing three major storms and geomagnetic quiet, respectively. We note that there was an inherent difficulty in the study in that the interplanetary spacecraft (Pioneer 10) was at 2.2 AU from the Sun and at a slightly different solar longitude than that of the Earth, and this required calculations of radial and corotation delays to match the spacecraft and event times. It is our hypothesis that there is little or no magnetic reconnection during northward interplanetary magnetic fields and that solar wind coupling occurs primarily during southward IMFs. This is in agreement with the conclusions of the references above. However, the timing of the relationship between interplanetary southward and northward magnetic fields and storm main phases should be revisited, especially when the measurements are not direct ones.

[6] In this paper, we study a major storm during 21–22 January 2005 that occurred during northward IMFs. We use the ACE and Cluster near-Earth monitors to identify solar wind features that impinge upon the magnetosphere. Through correlation analyses of the solar wind dawn-dusk electric field and SYM-H, we investigate the processes of solar wind energy input and energy release to the ring current during southward/northward IMF conditions.

2. Data Analysis

[7] An X 7.1 solar flare occurred at 0636 UT on 20 January 2005. The location was N14W61. The ICME associated with this flare arrived at the Earth ~34 h later. An SSC began at ~1712 UT on 21 January 2005 followed by a geomagnetic storm with a Dst maximum perturbation of −105 nT. Figure 1 shows the orbit of near-Earth satellites (Cluster C1, GEOTAIL, GOES10, GOES12, LANL 90 and LANL 97) during the period of a storm. The data from those satellites as well as ACE are used to study this event. ACE is located at L1, at a distance of X_{GSE} ~223 R_E and Y_{GSE} = ~−35.5 R_E. Time tags indicate the position of the satellites during different portions of the storm main phase.

2.1. Solar Wind Parameters and Geomagnetic Activity

[8] In Figure 2, the top seven panels are interplanetary ACE data. From top to bottom are: the ion temperature, *Tp*, the solar wind velocity, *Vsw,* the proton number density, *Np*, IMF magnitude, B_T, and components *Bx*, *By* and *Bz* in both GSM (in black) and GSE (in blue) coordinates from the ACE data. The instruments and the spacecraft are described by *Stone et al.* [1998]. In this figure, the data from the ACE satellite were shifted by 24 min to take into account solar wind convection delays between the ACE and Cluster satellite. It should be noted that this offset was set for the peak solar wind speed. Solar wind features that occur during lesser speeds should be delayed by greater amounts. The latter corrections were not made in this figure. Panels 8 through 10 are the Cluster C1 IMF components (*Bx*, *By* and *Bz* in GSM and GSE coordinates). Cluster was situated in the solar wind at (X~16 R_E and Y~10R_E). In general, the large scale features of the IMF components observed by ACE at L1 are quite similar to those observed by Cluster C1 located just in front of bow shock. In addition, it is noted that the *Bz*, *By* values in both GSM and GSE coordinates are very close for this time period. Thus we have confidence that the IMF features used are indeed those that impinged upon the magnetosphere during the storm.

[9] The bottom two panels of Figure 2 display the 1 min resolution AE and SYM-H indices. The 1-min-resolution SYM-H index, which is essentially the same as the hourly Dst index [*Sugiura and Poros*, 1971] except in terms of the time resolution, does not show any statistically significant development after the onset of substorms [*Iyemori and Rao*, 1996]. We used the SYM-H index only because of its high time rsolution. The solar wind pressure fluctuations are extremely large in this event, and could perhaps significantly influence the SYM-H measurements. More discussion on this topic will follow shortly. We plot the pressure-corrected SYM-H indices (SYM-H*) over the SYM-H at the bottom panel of Figure 2. SYM-H* is shown in red.

[10] A simple relationship [*Burton et al.*, 1975; *Gonzalez et al.*, 1989] is used to obtain SYM-H*:

$$\text{SYM-H}^* = \text{SYM-H} - b\sqrt{Dp} + c$$

where the constant c = 22 nT and b = 0.31 nT(eV cm-2)1/2 = 10.5 nT(nPa)1/2. SYM-H* is different from SYM-H near the SSC. However, it should be noted that the main phase growth starts at ~1946 UT as seen from SYM-H and SYM-H*.

[11] It is noted that SYM-H* is generally more negative than SYM-H, as expected. The maximum storm SYM-H is now −101 nT. It should also be noted that the correlation between northward IMF and the storm main phase is still present.

[12] An interplanetary shock is observed by ACE at ~1648 UT and by Cluster at ~1712 UT on 21 January 2005 (marked with an "S"). This shock and the enhanced southward IMF *Bz* in the following sheath induce the decrease of SYM-H to ~−41 nT. The solar wind velocity jumps from ~565 km/s to ~894 km/s across the shock. An unusual double-discontinuity, characterized by a non-compressive density enhancement (NCDE) [*Foullon et al.*, 2007], arrives at ~1843 UT on day 21, causing a second SI+/SSC at 1900 UT. This discontinuity is indicated by a vertical dotted line labeled D. The southward IMF *Bz* in the solar wind following the discontinuity led to the initial phase of the storm. The onset of the main phase begins at ~1946 UT.

[13] Detailed analyses of the ACE shock and the double-discontinuity were done to determine the details of these interplanetary structures which were responsible for the two geomagnetic SI+ events. Both structures were found to be highly unusual. The shock normal was determined by both the magnetic coplanarity [*Colburn and Sonnett*, 1966] and the Abraham-Shrauner [*Abraham-Shrauner and Yun*, 1976] mixed mode techniques. The shock velocity was calculated by assuming the Rankine-Hugoniot conservation relationships. The shock was found to be quasi-perpendicular with θ_{Bn} (the angle between the shock normal and the upstream magnetic field) determined to be 54° for both techniques. The Alfven and magnetosonic Mach numbers were 7.1 and

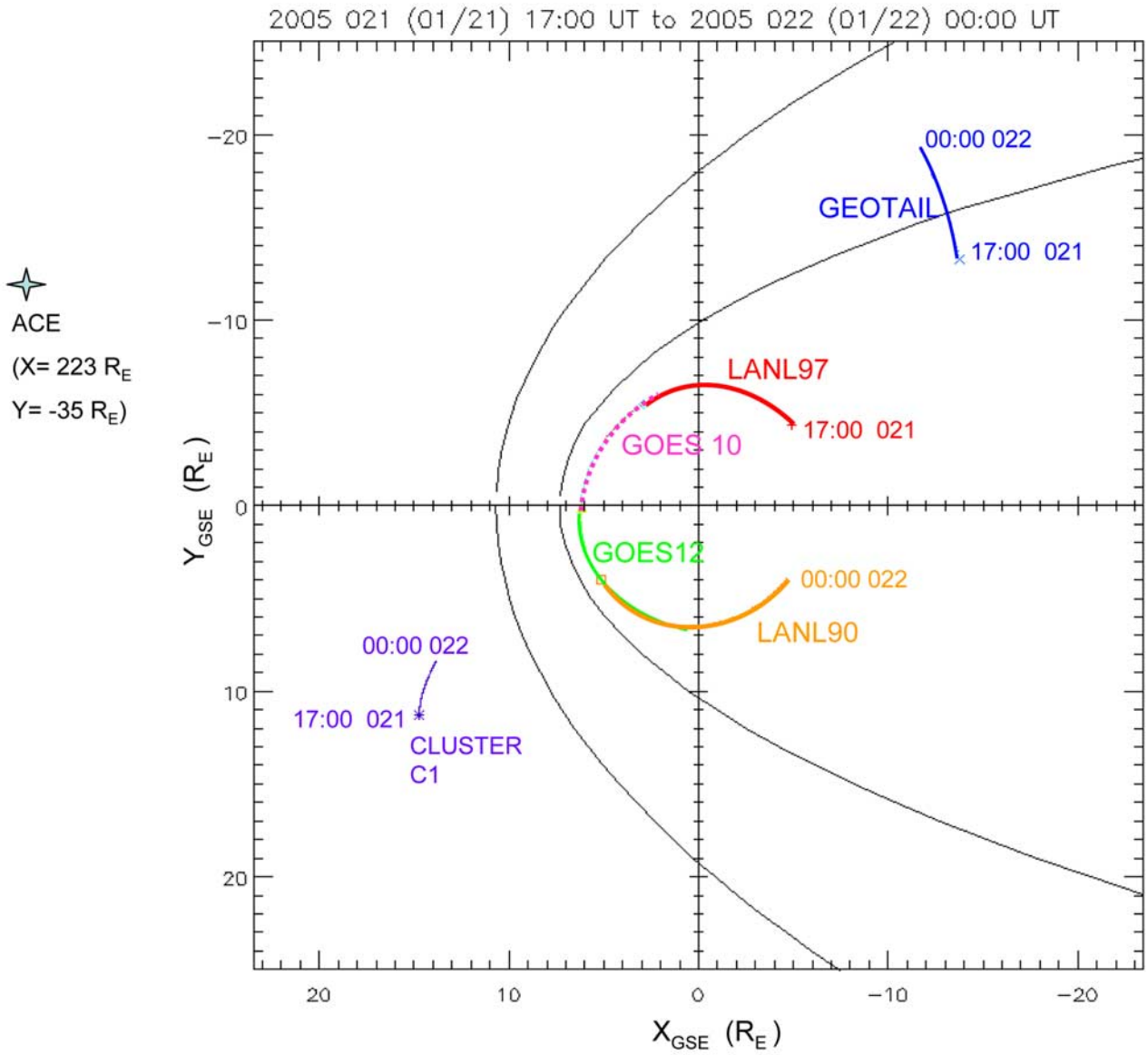

Figure 1. The orbit of the Cluster C1, GEOTAIL, GOES10, GOES12, LANL09 and LANL 97 satellites in the interval 1200 UT on day 21∼0800 UT on day 22, 2005.

5.4, respectively. These are extremely high values. Typical interplanetary (magnetosonic) shock Mach numbers at 1 AU range between 1.0 and 3.0 [*Tsurutani and Lin*, 1985]. They are rarely found above 4.0. This shock had a downstream overshoot, as expected for a shock of this type. Care was taken to avoid this region in the analyses. One might expect this strong shock event to cause unusual particle acceleration (but this is beyond the scope of the present paper).

[14] The double-discontinuity is also unusual. The minimum variance technique [*Tsurutani and Ho*, 1999] was used for the normal determination. The first discontinuity at 1815 UT had a normal angle of 83° relative to the interplanetary magnetic field. This is consistent with a tangential discontinuity or TD [*Landau and Lifschitz*, 1960]. The second discontinuity at 1817 UT had a normal direction of 74° relative to the ambient magnetic field direction, again a TD. These two TD are nearly parallel to each other. What is particularly interesting is that the pair of these magnetic discontinuities bound a single discontinuity in the solar wind density and temperature parameters. The solar wind proton density increases from 13/cm^{-3} to 45/cm^{-3} and the proton temperature decreases from 5.6 × 10^5 K to ∼4.0 × 10^5 K. The exact nature of this double-discontinuity is not certain at this time. Further work using multisatellite data will be needed to make further progress (the authors wish to thank E. Echer of INPE for help in these analyses. The reader is referred to the *Foullon et al.*, 2007 for analyses of the CLUSTER shock and double-discontinuity events).

[15] At ∼1946 UT (marked by a vertical line labeled M1), the IMF Bz turned northward. In the interval from 1946 UT to ∼2101 UT, the SYM-H sharply decreased to ∼ −90 nT, and the main phase of the storm began. At ∼2101 UT (marked by a vertical line labeled M2), the IMF fluctuates with small southward *Bz* components. It is also noted that *Bx* changed from a sunward to an antisunward direction, and then turned

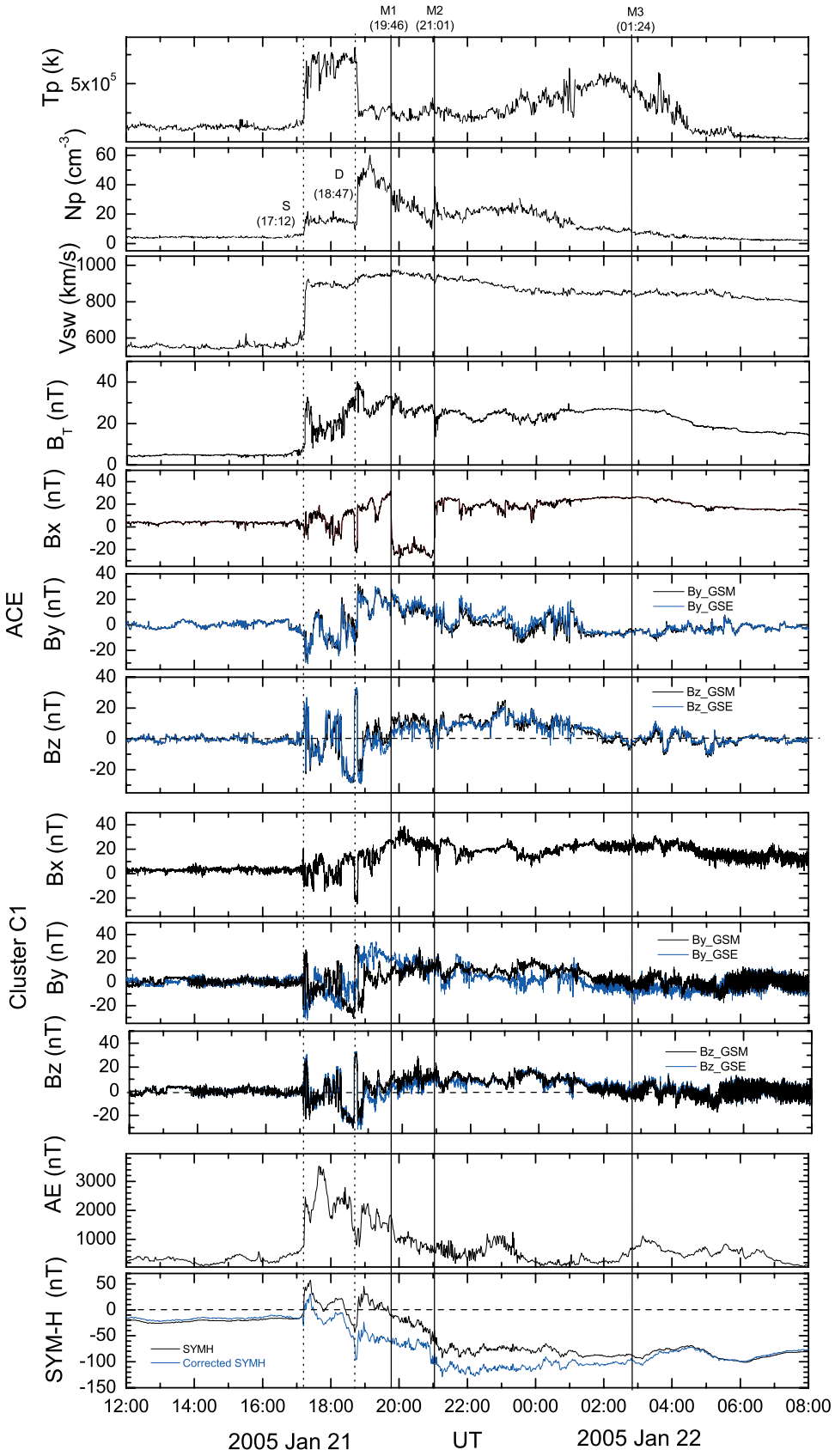

Figure 2. Interplanetary plasma and magnetic field data, AE and SYM-H geomagnetic index for the interval 21–22 January 2004. A shock (S), a discontinuity (D), the onset of the main phase (M1), and the duration of the northward IMF (M2 and M3) are indicated.

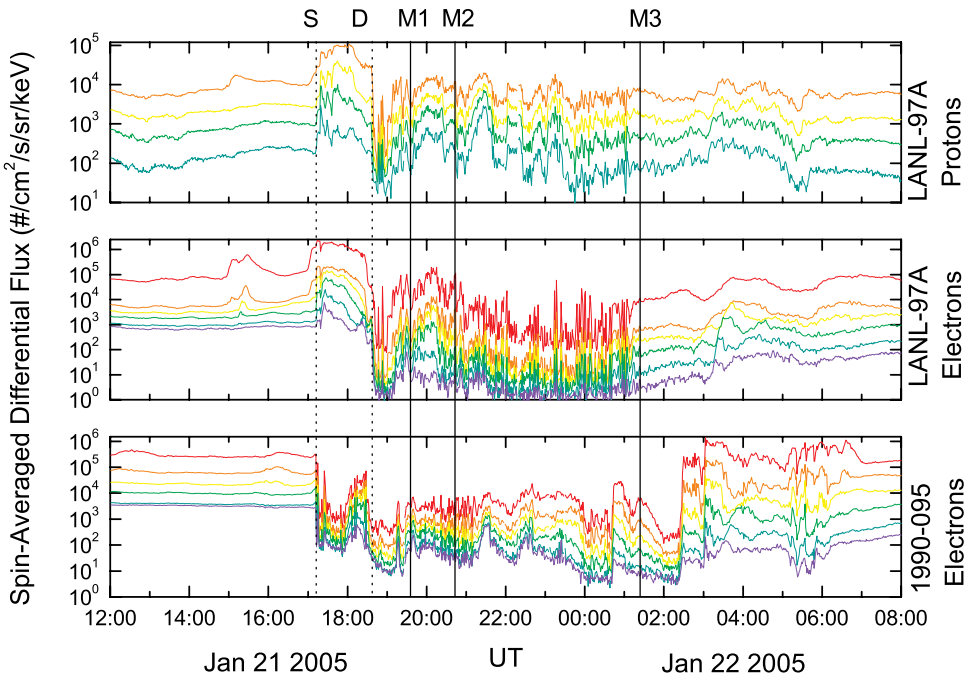

Figure 3. Los Alamos National Laboratory (LANL) energetic electron and proton data from two geosynchronous spacecraft LANL 1990–095 and LANL-1997A: Protons with energies (from orange to blue) 75–113 keV, 113–170 keV, 170–250 keV, 250–400 keV. Electrons with energies (from red to blue) 50–75 keV, 75–105 keV, 105–150 keV, 150–225 keV, 225–315 keV, 315–500 keV.

sunward again at ~2101 UT. The sharp IMF *Bx* changes (discontinuities) are not accompanied by *By* changes. Thus these discontinuities do not appear to be the heliospheric current sheet (HCS [*Smith et al.*, 1978]) crossings.

[16] From 2101 UT 21 January to 0124 UT 22 January (the vertical line labeled M3), *Bz* is small and positive (state rough values of ~10 nT). SYM-H is relatively stable at ~−80 nT. It indicates the development and maintenance of the symmetric ring current within the northward IMF event.

[17] In the interval 0124 to ~0612 UT, the IMF components fluctuated with southward Bz between ~±10 nT. At 0612 UT, SYM-H reached a minimum value of ~−101 nT, and the recovery phase of the storm began.

[18] It should also be noted that the AE index was generally low (<500 nT) during the storm main phase. This will be discussed below.

2.2. Observations of Magnetic Fields and Particle at Synchronous Orbit

[19] Figure 3 shows the Los Alamos National Laboratory (LANL) SOPA energetic proton and electron spin-averaged differential flux measurements from the LANL-90 and LANL-97 satellites during the interval of 21–22 January 2005.

[20] Between 21 January 1847 UT and 22 January 0124 UT, the energetic proton fluxes increased intermittently, keeping nearly the same level during the main phase of the storm. However, the fluctuations in the energetic electron fluxes decreased during this same period.

[21] Figure 4 shows that the magnetic fields and the magnetic tilt angles which are observed by GEOTAIL, and the GOES 10 and GOES 12 satellites. As is shown in Figure 1, GEOTAIL moved from the tail lobe into the magneto sheath, and the GOES 10 and GOES 12 satellites were located in morning and afternoon sectors of the outer magnetosphere, respectively. During the interval 1851~2010 UT (marked by vertical lines), the tilt angles rotated between ~−45° to ~+45° two times: this was mainly caused by the variation of Bz (seen in GEOTAIL). This indicates that the magnetic field in the plasma sheet changed from tailed-like to dipolar configuration corresponding to substorm activities. The AE index increased when IMF turns northward, and decreased when the IMF turned southward as shown in Figure 2. In the same period, the energetic proton fluxes increased two times as shown in Figure 3. From ~2010 UT to ~2000 UT, the tilt angles increased and to values about 90°. After ~2000 UT, the tilt angles slowly decreased. One suggestion is that the magnetic field depolarized slowly without expansion onsets. Unfortunately, no magnetotail data of the magnetic field are available for this event.

3. Discussion

[22] During the storm of 21–22 January 2005, the southward magnetic field in the sheath following the shock at ~1712 UT led to the decrease of SYM-H with a peak around ~−41 nT at 1847 UT. The storm initial phase was started by the sudden increased ram pressure behind the fast shock. The higher plasma density and higher velocity combined to form a much larger solar wind ram pressure.

[23] The increased ram pressure behind a discontinuity at ~1847 UT induced a second SI+/SSC. Southward magnetic field followed this discontinuity leading to a second decrease of SYM-H. However, during the storm main phase, the IMF

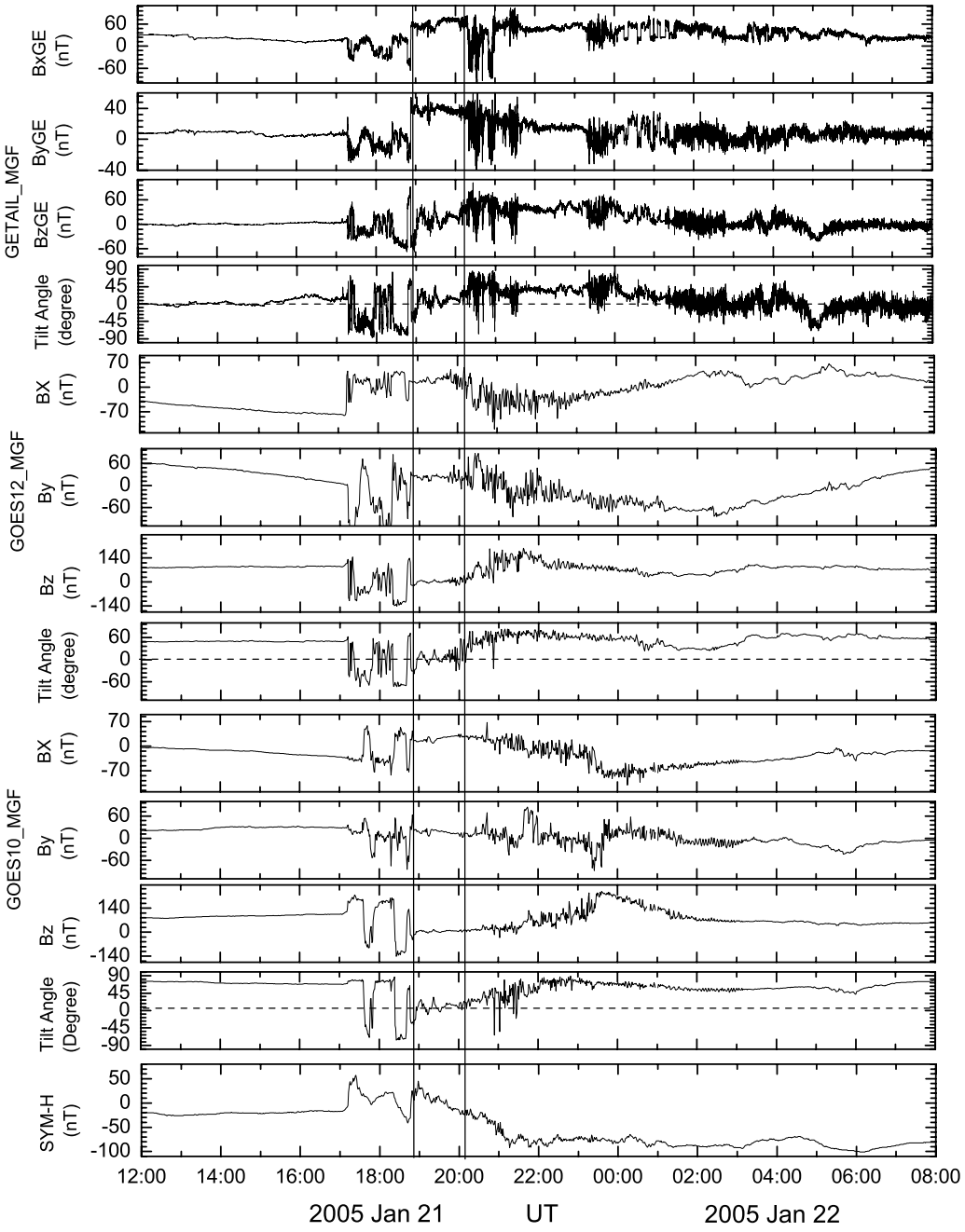

Figure 4. The magnetic fields and the magnetic tilt angles observed by GEOTAIL, GOES 10 and GOES 12 satellites.

Bz turned northward. Northward IMFs dominated the storm main phase from ~1946 UT to 0124 UT.

[24] The energy supplied by the solar wind was initially converted to electromagnetic energy (and can be viewed as to be stored in the magnetic field, primarily the magnetotail) [*Kamide et al.*, 1998]. Delayed energy release (after storage) may be possible [*Tsurutani and Gonzalez*, 1995]. The measurements from GEOTAIL [*Nishida*, 1994] confirmed the importance of a solar wind source for energetic ions in the magnetotail, especially for distances greater than ~30 R_E [*Christon et al.*, 1996; *Daglis et al.*, 1999]. Investigation of combined measurements from the Wind and GEOTAIL spacecraft [*Terasawa et al.*, 1997; *Daglis et al.*, 1999] showed that for extended periods of northward IMF, that is, during geomagnetically quite times, the magnetotail at distances beyond 15 R_E is dominated by solar wind particles entering through the flank regions. However, the effective source geometry of the solar wind, where and how solar wind particles enter the magnetosphere, remains an open question [*Daglis et al.*, 1999].

[25] It is generally assumed that the accumulation of energy in the ring current would be linearly related to the accumulation of input energy from the solar wind. We employ the integrated interplanetary electric field *Ey* (ΣEy) to represent the accumulation of input energy from the solar wind where $Ey = -V \times Bs$, V is solar wind speed

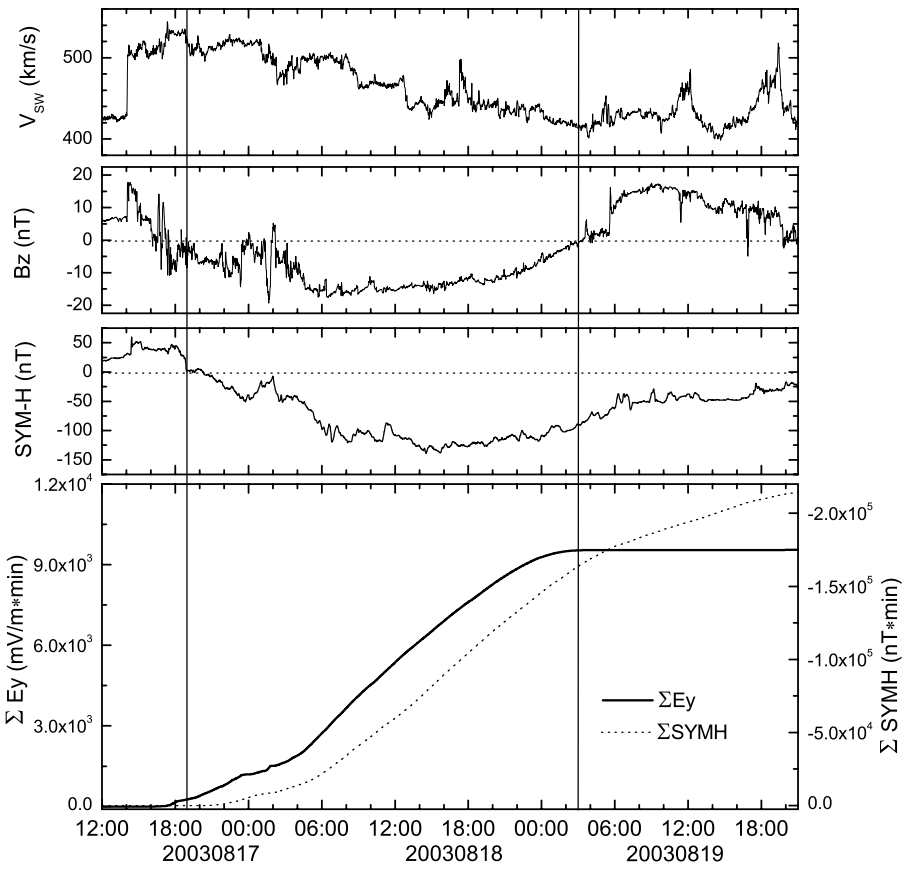

Figure 5. An example of a southward IMF storm event on 17–19 August 2003.

and $Bs = -Bz$ if IMF $Bz < 0$; $Bs = 0$ if IMF $Bz >= 0$. The integrated SYM-H (ΣSYMH) is applied to represent the release of energy into the ring current.

[26] For comparative purposes, we have analyzed another magnetic storm in the same fashion. The event during 17–19 August 2003 has been selected due to its typical fast response to southward IMF Bzs. The upper three panels in Figure 5 show the solar wind speed, the IMF *Bz* and the SYM-H indices. The bottom panel shows Σ*Ey* and ΣSYMH as a function of time. It is found that ΣSYMH increases almost linearly with the increase of Σ*Ey* during the main phase. One interpretation is that this storm belongs to the "directly driven" type. The energy dissipates at a rate faster than it was stored [*Baker et al.*, 1985], so that the previously loaded energy is rapidly unloaded.

[27] Figure 6 shows the temporal variations of Σ*Ey* and ΣSYMH for the storm of 21–22 January 2005 which is the focus of this paper. During a quiet period preceding the storm (1200 UT ~1712 UT), the slopes of both Σ*Ey* and Σ*SYMH* remain nearly constant with small values and can be thought of as being linearly correlated. It indicates that energy input from the solar wind and energy released in the ring current are very low. As is shown in Figure 4, the tilt angles of the magnetic field at synchronous orbit in the magnetosphere were kept to be near 80°. This is a stable configuration during quite time.

[28] During 1712~1850 UT, the Σ*Ey* increased sharply with a high slope, while Σ*SYMH* still continue to increase slowly and its slope did not change much. Our interpretation is that a large amount of solar wind energy had entered into the magnetosphere due to the prior southward IMF *Bz*. It is our conjecture that at this time not much energy was released into the ring current, only a contribution to substorm activities, as is shown by the AE index. This magnetotail energy storage may arise from intense dynamic pressure by shock and discontinuity impacting the magnetosphere, restricting the development of the ring current and partial ring current causing the main phase of a storm. We note that the tilt angle of the magnetic field jumped between positive and negative values twice, which may correspond to the onset of substorms.

[29] After 1850 UT, Σ*Ey* stayed constant for a long time until 0140 UT of day 22 due to northward IMF *Bz*. However, the tilt angle of magnetic field was near zero during 1850~1946 UT which indicates a distorted and stretched magnetospheric configuration. It also means that a part of input solar wind energy might be stored in magnetosphere with the form of magnetic energy. This period of 1850~1946 UT with tilt angle of near zero value can be regarded as "the energy storing phase."

[30] From 1946 UT to 0140 UT of day 22, Σ*SYMH* increased sharply, while Σ*Ey* remained unchanged. The slope of Σ*SYMH* steepened but the slope of Σ*Ey* stayed near zero. The tilt angle of magnetic field gradually increased to 80° for a stable magnetospheric configuration. This may indicate that the magnetic energy stored in the magnetosphere is converted to kinetic energy of particles in the ring current although there is little or no input energy

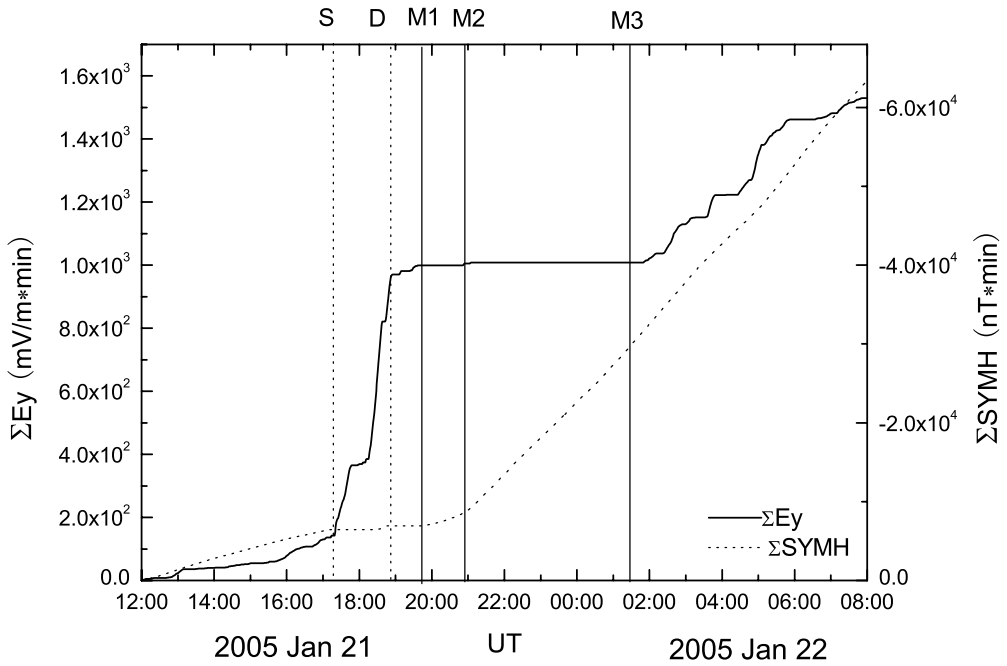

Figure 6. The temporary variation for the integration of Ey and SYM-H in the interval 20–21 January 2005.

from the solar wind due to northward IMF *Bz*. The period of 1850∼0140 UT can be called as "the energy releasing phase." It is like a "slowly unloading process."

[31] After 0140 UT on day 22, the slopes of Σ*Ey* and Σ*SYMH* resumed the slow increase of the quiet time prior the storm. The magnetosphere recovered to a stable configuration with the tilt angle of near 80°.

4. Final Comments

[32] During the storm event on 21 January 2005 there are high solar wind velocities, a large Mach 5.4 shock followed by a double-discontinuity (bounding a NCDE), and an interval of long-duration ∼+10 nT northward IMF during the storm main phase. Using interplanetary and magnetospheric satellite data, we have interpreted this as a lengthy storage of solar wind energy in the magnetotail and delayed release into the ring current.

[33] Other possible scenarios exist. Substantial magnetic reconnection could be taking place during these small northward IMFs, leading to plasma sheet injection into the nightside magnetosphere and tail energy accumulation. The plasma sheet may thus be close to the Earth in this case, resulting in a large contribution of tail current to the SYM-H index [*Pulkkinen et al.*, 1994; *Baker et al.*, 2001; *Turner et al.*, 2000; *Feldstein et al.*, 2005]. Additionally contributions from "viscous interaction" mechanisms should be studied as well.

[34] We of course do not have a definitive answer for the mechanism for this anomalous IMF northward magnetic storm event. We encourage others to find and investigate events like these to better understand such cases, even though they occur only a small percentage of the time.

[35] **Acknowledgments.** We appreciate discussions with Gordon Rostoker. We acknowledge the CDAWeb for access to the Cluster, Wind, GOES10 and GOES12 data. SOPA energetic proton and electron spin-averaged differential flux measurements are afforded by Los Alamos National Laboratory. The SYMH, AE data are provided by the World Data Center for Geomagnetism at Kyoto University. This work was supported by MOST 973 Plan (2006CB806305) and NSFC (40774086). Portions of the work were performed at the Jet Propulsion Laboratory, California Institute of Technology, under contract with NASA.

[36] Zuyin Pu thanks Zdenka Smith and another reviewer for their assistance in evaluating this paper.

References

Abraham-Shrauner, B., and S. H. Yun (1976), Interplanetary shocks seen by Ames plasma probe on Pioneer 6 and 7, *J. Geophys. Res.*, *81*(13), 2097, doi:10.1029/JA081i013p02097.

Akasofu, S.-I. (1981a), Energy coupling between the solar wind and the magnetosphere, *Space Sci. Rev.*, *28*, 121, doi:10.1007/BF00218810.

Akasofu, S.-I. (1981b), Prediction of development of geomagnetic storms using the solar wind-magnetosphere energy coupling function, *Planet. Space Sci.*, *29*, 1151, doi:10.1016/0032-0633(81)90121-5.

Axford, W. I., and C. O. Hines (1961), A unifying theory of high-latitude geophysical phenomena and geomagnetic storms, *Can. J. Phys.*, *39*, 1433.

Baker, D. N., T. A. Fritz, R. L. McPherron, D. H. Fairfield, Y. Kamide, and W. Baumjohann (1985), Magnetotail energy storage and release during the CDAW 6 substorm analysis intervals, *J. Geophys. Res.*, *90*, 1205–1216, doi:10.1029/JA090iA02p01205.

Baker, D. N., N. E. Turner, and T. I. Pulkkinen (2001), Energy transport and dissipation in the magnetosphere during geomagnetic storms, *J. Atmos. Sol. Terr. Phys.*, *63*, 421, doi:10.1016/S1364-6826(00)00169-3.

Burton, R. K., R. L. McPherron, and C. T. Russell (1975), An empirical relationship between interplanetary conditions and Dst, *J. Geophys. Res.*, *80*, 4204, doi:10.1029/JA080i031p04204.

Christon, S. P., G. Gloeckler, D. J. Williams, R. W. McEntire, and A. T. Y. Lui (1996), The downtail distance variation of energetic ions in Earth's magnetotail region: GEOTAIL measurements at $X > -208\ R_E$, *J. Geomag. Geoelectr.*, *48*, 615–627.

Colburn, D. S., and C. P. Sonnett (1966), Discontinuities in the solar wind, *Space Sci. Rev.*, *5*, 439, doi:10.1007/BF00240575.

Daglis, I. A., R. A. Thorne, W. Baumjohann, and S. Orsini (1999), The terrestrial ring current: Origin, formation, and decay, *Rev. Geophys.*, *37*, 407–438, doi:10.1029/1999RG900009.

Dungey, J. W. (1961), Interplanetary magnetic field and the auroral zones, *Phys. Rev. Lett.*, *6*, 47–48, doi:10.1103/PhysRevLett.6.47.

Echer, E., W. D. Gonzalez, and B. T. Tsurutani (2008a), Interplanetary conditions leading to superintense geomagnetic storms (Dst ≤ -250 nT) during solar cycle 23, *Geophys. Res. Lett.*, *35*, L06S03, doi:10.1029/2007GL031755.

Echer, E., W. D. Gonzalez, B. T. Tsurutani, and A. L. C. Gonzalez (2008b), Interplanetary conditions causing intense geomagnetic storms (Dst ≤ -100 nT) during solar cycle 23 (1996–2006), *J. Geophys. Res.*, *113*, A05221, doi:10.1029/2007JA012744.

Feldstein, Y. I., et al. (2005), Self-consistent modeling of the large-scale distortions in the geomagnetic field during the 24–27 September 1998 major magnetic storm, *J. Geophys. Res.*, *110*, A11214, doi:10.1029/2004JA010584.

Foullon, C., C. J. Owen, S. Dasso, L. M. Green, I. Dandouras, H. A. Elliott, A. N. Fazakerley, Y. V. Bogdanova, and N. U. Crooker (2007), Multi-spacecraft study of the 21 January 2005 ICME: Evidence of current sheet substructure near the periphery of a strongly expanding, fast magnetic cloud, *Sol. Phys.*, *244*, 139–165, doi:10.1007/s11207-007-0355-y.

Gonzalez, W. D., and B. T. Tsurutani (1987), Criteria of interplanetary parameters causing intense magnetic storms (DST < -100 nT), *Planet. Space Sci.*, *35*, 1101, doi:10.1016/0032-0633(87)90015-8.

Gonzalez, W. D., B. T. Tsurutani, A. L. C. Gonzalez, E. J. Smith, F. Tang, and S. I. Akasofu (1989), Solar wind-magnetosphere coupling during intense magnetic storms (1979–1979), *J. Geophys. Res.*, *94*, 8835, doi:10.1029/JA094iA07p08835.

Gonzalez, W. D., J. A. Joselyn, Y. Kamide, H. W. Kroehl, G. Rostoker, B. T. Tsurutani, and V. M. Vasyliunas (1994), What is a geomagnetic storm?, *J. Geophys. Res.*, *99*, 5771–5792, doi:10.1029/93JA02867.

Gonzalez, W. D., E. Echer, A. L. Clua-Gonzalez, and B. T. Tsurutani (2007), Interplanetary origin of intense geomagnetic storms (Dst < -100 nT) during solar cycle 23, *Geophys. Res. Lett.*, *34*, L06101, doi:10.1029/2006GL028879.

Iyemori, T., and D. R. K. Rao (1996), Decay of the Dst field of geomagnetic disturbance after substorm onset and its implication to storm-substorm relation, *Ann. Geophys.*, *14*, 608–618, doi:10.1007/s00585-996-0608-3.

Kamide, Y., et al. (1998), Current understanding of magnetic storms: Storm-substorm relationships, *J. Geophys. Res.*, *103*, 17,705–17,728, doi:10.1029/98JA01426.

Lamb, S. H. (1945), *Hydrodynamics*, 6th ed., Cambridge Univ. Press, New York.

Landau, L. D., and E. M. Lifschitz (1960), *Electrodynamics of Continuous Media*, 255 pp., Pergamon, Tarrytown, N. Y.

Nishida, A. (1994), The GEOTAIL mission, *Geophys. Res. Lett.*, *21*, 2871–2873, doi:10.1029/94GL01223.

Pulkkinen, T. I., D. N. Baker, D. G. Mitchell, R. L. McPherron, C. Y. Huang, and L. A. Frank (1994), Thin current sheets in the magnetotail during substorms: CDAW 6 revisited, *J. Geophys. Res.*, *99*, 5793, doi:10.1029/93JA03234.

Smith, E. J., and J. H. Wolfe (1976), Observations of interaction regions and corotating shocks, *Geophys. Res. Lett.*, *3*, 137–140, doi:10.1029/GL003i003p00137.

Smith, E. J., B. T. Tsurutani, and R. L. Rosenberg (1978), Observations of the interplanetary sector structure up to heliographic latitudes of 16 Pioneer 11, *J. Geophys. Res.*, *83*, 717, doi:10.1029/JA083iA02p00717.

Stone, E. C., A. M. Frandser, R. A. Mewaldt, E. R. Christian, D. Margolies, J. F. Ormes, and F. Snow (1998), The advanced composition explorer, *Space Sci. Rev.*, *86*, 1–22, doi:10.1023/A:1005082526237.

Sugiura, M., and D. N. Poros (1971), *NASA Rep., X-645-71-278*.

Terasawa, T., et al. (1997), Solar wind control of density and temperature in the near-Earth plasma sheet: Wind/Geotail collaboration, *Geophys. Res. Lett.*, *24*, 935–938, doi:10.1029/96GL04018.

Tsurutani, B. T., and W. G. Gonzalez (1995), The efficiency of viscous interaction between the solar wind and the magnetosphere during intense northward IMF events, *Geophys. Res. Lett.*, *22*, 663–666, doi:10.1029/95GL00205.

Tsurutani, B. T., and C. M. Ho (1999), A review of discontinuities and Alfven waves in interplanetary space: Ulysses results, *Rev. Geophys.*, *37*, 517–541, doi:10.1029/1999RG900010.

Tsurutani, B. T., and R. P. Lin (1985), Acceleration of >47 keV ions and >2 keV electrons by interplanetary shocks at 1 AU, *J. Geophys. Res.*, *90*, 1, doi:10.1029/JA090iA01p00001.

Tsurutani, B. T., and R. M. Thorne (1982), Diffusion processes in the magnetopause boundary layer, *Geophys. Res. Lett.*, *9*, 1247–1250, doi:10.1029/GL009i011p01247.

Tsurutani, B. T., W. D. Gonzalez, F. Tang, S. I. Akasofu, and E. J. Smith (1988), Origins of interplanetary southward energetic fields responsible for major magnetic storms near solar maximum (1978–1979), *J. Geophys. Res.*, *93*, 8519, doi:10.1029/JA093iA08p08519.

Tsurutani, B. T., W. D. Gonzalez, F. Tang, Y. T. Lee, M. Okada, and D. Park (1992), Great magnetic storms, *Geophys. Res. Lett.*, *19*, 73–76, doi:10.1029/91GL02783.

Tsurutani, B. T., W. D. Gonzalez, X.-Y. Zhou, R. P. Lepping, V. Bothmer, and J. Atmosph (2004), Properties of slow magnetic clouds, *Sol. Terr. Phys.*, *66*, 147, doi:10.1016/j.jastp.2003.09.007.

Turner, N. E., N. Baker, T. I. Pulkkinen, and R. L. McPherron (2000), Evaluation of the tail current contribution to Dst, *J. Geophys. Res.*, *105*, 5431, doi:10.1029/1999JA000248.

A. M. Du, Institute of Geology and Geophysics, Chinese Academy of Sciences, Beijing 100029, China. (amdu@mail.igcas.ac.cn)

W. Sun, Geophysical Institute, University of Alaska Fairbanks, Fairbanks, AK 99775, USA.

B. T. Tsurutani, Jet Propulsion Laboratory, California Institute of Technology, Pasadena, CA 91109, USA.